NANO LETTERS

2007
Vol. 7, No. 11
3523−3527

Plasmon-Assisted Local Temperature Control to Pattern Individual Semiconductor Nanowires and Carbon Nanotubes

Linyou Cao, David N. Barsic, Alex R. Guichard, and Mark L. Brongersma*

Department of Materials Science and Engineering, Geballe Laboratory for Advanced Materials, Stanford University, Stanford, California 94305

Received September 4, 2007; Revised Manuscript Received September 30, 2007

ABSTRACT

We demonstrate a new versatile strategy to rapidly heat and cool subdiffraction-limited volumes of material with a focused light beam. The local temperature rise is obtained by exploiting the unique optical properties of metallic nanostructures that facilitate efficient light-to-heat conversion through the excitation of surface plasmons (collective electron oscillations). By locally heating nanoscale metallic catalysts, growth of semiconductor nanowires and carbon nanotubes can be initiated and controlled at arbitrarily prespecified locations and down to the single nanostructure level in a room-temperature chamber. This local heating strategy can be orders of magnitude (>10^5) more energy efficient than conventional chemical vapor deposition (CVD) tools in which an entire chamber/substrate is heated. For these reasons, it has great potential for use in process- and energy-efficient assembly of nanowires into complementary metal-oxide-semiconductor (CMOS) compatible device architectures. In general, the high degree of spatial and temporal control over nanoscale thermal environments afforded by this method inspires new pathways for manipulating a range of important thermally stimulated processes and the development of novel photothermal devices.

The realization of controlled, nanoscale thermal environments has great fundamental and practical importance.[1,2] Research in this area is largely driven by a desire to better control and monitor physicochemical[3−5] or biochemical reactions[6,7] and to develop thermally controlled nanoscale devices.[8] In particular, thermally stimulated, local growth of nanostructures and devices has recently attracted significant attention.[9−11] If such methods were to provide exquisite control over the growth location, speed, and orientation of nanostructures, it would greatly increase their applicability in complex device architectures anticipated in the Semiconductor Industry Association (SIA) roadmap.[12] Most semiconductor nanowires (NWs) and carbon nanotubes (CNTs) are currently grown by a metal-catalyzed chemical vapor deposition (CVD) technique in a globally heated furnace. Such procedures can damage pre-existing device structures, and hence device fabrication typically requires laborious postgrowth processing.

The optical properties of metallic nanostructures have long been harnessed to enable routing and manipulation of light at the nanoscale.[13−15] This high degree of control over light-matter interactions is derived from the fact that nanostructured metals support light-induced surface plasmon (SP) excitations or collective electron oscillations.[16,17] In the chemical industry, metal nanostructures also play a vital role as catalysts and are used in bulk quantities. Merging of the fields of plasmonics and catalysis thus seems natural and extremely beneficial. In 1981, Nitzan and Brus already argued that the electromagnetic field concentration afforded by SPs should enhance the rate of photochemical reactions.[18] Soon thereafter, this was demonstrated by Chen and Osgood for the photodissociation of dimethyl cadmium.[19] More recently, the heat generated by rapid (<10 fs) SP damping in metals (Landau damping) was utilized to produce oxide depositions in micronscale areas[20] to grow metallic nanoparticles,[21] selectively identify and kill cancer cells,[6,22,23] obtain rippling of polymer surfaces,[24] and induce phase transitions.[25,26] In this letter, we demonstrate the use of metal nanoparticles to concentrate light into nanoscale regions (well below the diffraction limit) with the aim to generate truly nanometer-sized hotspots in which thermally activated processes such as the growth of nanowires or nanotubes can be initiated and controlled. The presented results show the technique has substantial implications for efficient integration of NWs or NTs into complex semiconductor device architectures.

The first set of experiments were performed by flowing a precursor gas over gold (Au) nanoparticle arrays on transparent fused silica substrates illuminated with a low-power

* E-mail: brongersma@stanford.edu. Tel: (650) 736-2152. Fax: (650) 725-4034.

10.1021/nl0722370 CCC: $37.00
Published on Web 10/27/2007

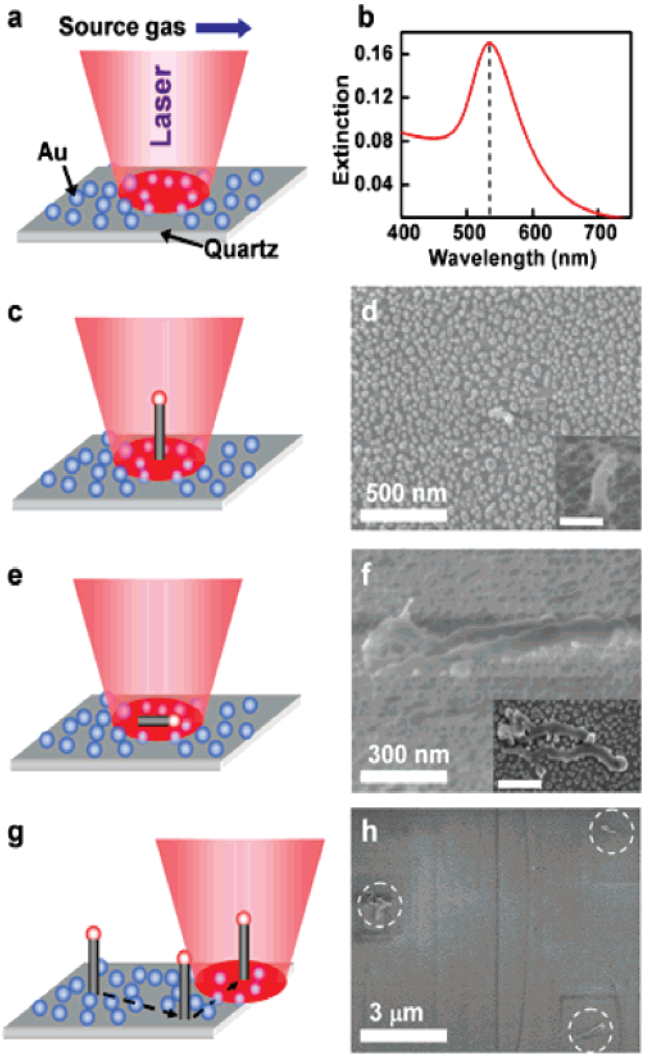

Figure 1. (a) Schematic illustration of the plasmon-assisted local temperature control procedure in which a low-power, continuous wave laser illuminates a transparent substrate coated with catalytically active, light-absorbing, metallic nanoparticles (catalyst). The metal nanoparticles rapidly heat up under the illuminating laser beam due to efficient, plasmon-assisted conversion of light to heat inside the particles. (b) Extinction spectrum of an array of Au particles on a fused quartz slide that exhibits a strong surface plasmon resonance around a wavelength of 530 nm (dashed vertical line). The random Au nanoparticle array was generated by annealing a 5 nm thick evaporated Au film in Ar for 10 min. (c,d) Schematic and top-view SEM image of a single Si nanowire surrounded by Au nanoparticles that have not catalyzed growth. The inset shows the same wire in a side view with a scale bar of 100 nm. (e,f) Schematic and side view SEM image of horizontally grown (in-plane) nanowires. The inset shows a top view SEM image of the same wires (scale bar is 200 nm). (g,h) Schematic indicating how individual nanowires can be patterned by moving the focused, illumination spot from one growth location to the next and corresponding SEM image of three patterned nanowires (located inside the white circles). Magnified SEM images of the nanowires in Figure 1h are shown in the Supporting Information (Figure S2).

density, continuous wave (CW) laser at a wavelength, $\lambda =$ 532 nm (Figure 1a). At this wavelength, Au nanoparticles exhibit a strong, characteristic peak in the light absorption due to a SP resonance (Figure 1b).[17] The absorbed light causes rapid local heating of the Au particle catalyst, allowing it to decompose the precursor gas and thereby initiate nanostructure growth. Reference experiments without metallic particles never resulted in nanostructure growth, even at an order of magnitude higher laser powers than used in the experiments below. We also verified that the use of illumination wavelengths slightly off the peak of surface plasmon resonance ($\lambda = 514$ and 632 nm) required noticeably higher powers to induce growth. Local growth of an individual Si NW was achieved using a 7.2 μm diameter Gaussian beam spot at 0.49 mW/μm^2 and 2% silane (SiH_4) in Ar, ~80 sccm under 80 Torr, as a precursor gas (Figure 1c,d). The growth of single NWs is quite challenging as it requires the preferential heating of one specific catalyst particle, while others need to remain at temperatures below a certain threshold required for growth. However, by carefully controlling the laser power, single NW growth in a local "hotspot" could be repeated many times in succession, and some examples are shown in the other scanning electron microscopy (SEM) images in Figure 1. The ability of random, metallic nanoparticle arrays and engineered metallic structures to repeatable generate nanoscale hotspots is explained in more detail in the discussion of our thermal model below. The illumination power density does need to be strictly limited to avoid simultaneous growth of a multitude of wires or even rampant uncatalyzed deposition at much higher power densities (see Supporting Information, Figure S1). It is important to note that the amount of light energy expended to grow this wire is about 0.90 J (20 mW laser power and 45 s illumination time). To our knowledge, this is the least amount of energy ever used to grow a NW, and it is suggestive of a highly energy-efficient pathway to fabricate devices employing a small number of single nanostructures. Conventional tube furnaces that expend at least 5 orders of magnitude more energy for a typical growth and offer less flexibility/precision in determining the growth location may still be preferred for deposition of large-area nanostructure arrays.

This technique also allows control over the growth direction of nanostructures. We discovered that the growth orientation of Si NWs is tunable to a certain extent by changing the degree of focusing of the illumination beam. We repeatedly found an increase in the number of horizontally grown (in-plane) Si NWs (Figure 1e,f) as the illumination spot size was decreased. We are hypothesizing that the lateral temperature gradient may play an important role in determining the growth direction, and we are currently verifying this hypothesis. If the observed control can be understood and further improved, it could have important implications for efficient integration of Si NWs into planar semiconductor devices.

The local photothermal heating strategy also offers a novel solution to the challenge of efficiently patterning nanostructures at prespecified locations, which has greatly restricted the application of NWs and CNTs in nanoscale devices so far. Individual Si NWs were grown at arbitrarily prespecified locations from a random array of Au nanoparticles by moving the laser beam from one growth spot to the next (Figure 1g,h). This flexible growth strategy could be repeated at an arbitrary number of places and the placement accuracy is

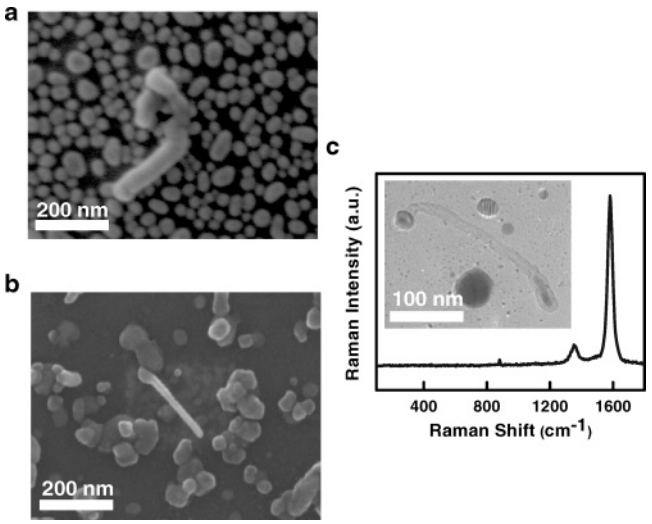

Figure 2. (a) Scanning electron microscopy (SEM) image of gold-catalyzed germanium nanowires. (b) SEM image of nickel-catalyzed silicon nanowires. In experiments, we observed that the nickel catalyst at the top of the nanowire was faceted, suggestive of a vapor−solid−solid growth mechanism. (c) TEM image of a multiwall CNT with an encapsulated catalyst inset into a Raman spectrum taken from the CNT growth region. The Raman spectrum shows two narrow line width peaks at 1352 and 1582 cm^{-1} that are characteristic of CNTs. The absence of the breathing mode peak at ∼100−200 cm^{-1} characteristic of single walled CNTs suggests a high fraction of multiwalled CNTs in the area probed with Raman.

only limited by the precision of the sample manipulation stage and/or the catalyst particle density. This process allows one to run large numbers of growth experiments in parallel by using a large area beam and existing optical masking technology. It also could significantly speed up device processing times and enable massive-scale, parallel, fundamental growth and catalysis studies.

The generality of this proposed approach to control chemical reactions and deposition was explored by investigating growth of other relevant nanosystems. When using a precursor gas of germane (GeH_4) rather than SiH_4, germanium (Ge) NWs were successfully grown with similar characteristics to those described above for the Si NWs (Figure 2a). Other catalysts besides Au were investigated as well. We found that even easily oxidized nanoparticles such as Ni, Ti, and Fe were able to catalyze Si deposition (Figure 2b). This implies that the CMOS compatible metal (e.g., Ni and Ti) silicide contacts to transistors on Si chips could directly be used as seeds for NW growth. Although some metals show strong plasmon resonances and other do not, the technique can be successfully applied as long as the absorption in the catalyst is substantially stronger than in the substrate. As further evidence for the generality of the technique, CNTs were also grown using a mixture of methane and ethylene as a source gas and Ni nanoparticles as the catalyst (see transmission electron microscopy (TEM) image in Figure 2c, inset). A Raman spectrum taken from the growth region shows two narrow line width peaks at 1352 and 1582 cm^{-1} that are characteristic of CNTs (Figure 2c).[27] The absence of a radial-breathing mode in the spectral region from 100 to 200 cm^{-1} indicates that most of the tubes are multiwall,[27] which is consistent with the TEM results. It is worthwhile to note that this method is potentially promising for chirality-controlled growth of individual CNTs based on recent reports suggesting that intense visible laser light can help select CNTs with specific chirality.[28]

To gain more quantitative insight into this temperature control technique, a thermal model has been constructed to calculate the temperature field and heating dynamics of the metal particles under the laser beam. When illuminated, each nanoparticle acts as a heat source that transfers thermal energy to its environment. For the growth temperatures described in this paper, heat transfer by conduction is dominant, while both radiation and convection are negligible. For the high-density metallic nanoparticle arrays used in this study, integral equations can be used to approximate the temperature distribution in the silica substrate under a Gaussian laser beam[29]

$$T(r,z,t) = \frac{fP}{K}\frac{D^{1/2}}{\pi^{3/2}}\int_0^t \frac{1}{\sqrt{t'}(4Dt' + r_0^2/2)} \exp\left(-\frac{z^2}{4Dt'} - \frac{r^2}{4Dt' + r_0^2/2}\right)dt' \quad (1)$$

where P is the laser power, f is the frequency-dependent absorbed fraction of the laser power, which is highest at the SP resonance. K and D are the thermal conduction coefficient and thermal diffusivity of the substrate, respectively, r_0 is the radius of the Gaussian laser beam described by $I(r) = I_0 \exp(-2r^2/r_0^2)$. The magnitude of z denotes the distance from the sample surface into the substrate. In this model, we disregard the temperature dependence of the thermal conductivity and diffusivity of the substrate. For fused silica glass, the temperature dependencies of these quantities are weak and we took the values at 400 °C (manufacturer's data), $K = 1.91$ W/m °C and $D = 8.05 \times 10^{-7}$ m^2/s respectively. The proposed thermal model predicts that the temperature at the surface of the silica substrate right in the center of the laser spot approaches a steady-state value equal to $T_C = fP/\sqrt{2/\pi}Kr_0$. It is thus clear that focusing light to smaller spot sizes helps in reaching higher temperatures. Due to the thermal resistance between the Au nanoparticles and the silica ($\sim 2.0 \times 10^{-8}$ W/m^2 °C) the local temperature in the particles is higher than the substrate by an amount equal to the heat flux times the thermal resistance.[30]

Our calculations in Figure 3a show that a tightly focused (e.g., $r_0 = 1$ μm) CW laser beam can easily generate temperatures required for catalysis/deposition (a few hundred degrees Celsius) with a power comparable to that of a simple laser pointer (a few mW). The efficient heating through the metallic nanoparticles is a direct consequence of their strong, resonantly enhanced absorption associated with the SP resonance effect. The calculations also show that the high temperatures in the substrate (hot zone) are confined to a volume that is approximately the beam radius cubed, r_0^3 (Figure 3b). For this reason, fragile device structures in close proximity of the illuminated region will not be affected by the high temperatures. This further illustrates why plasmon-assisted temperature control may provide a promising route

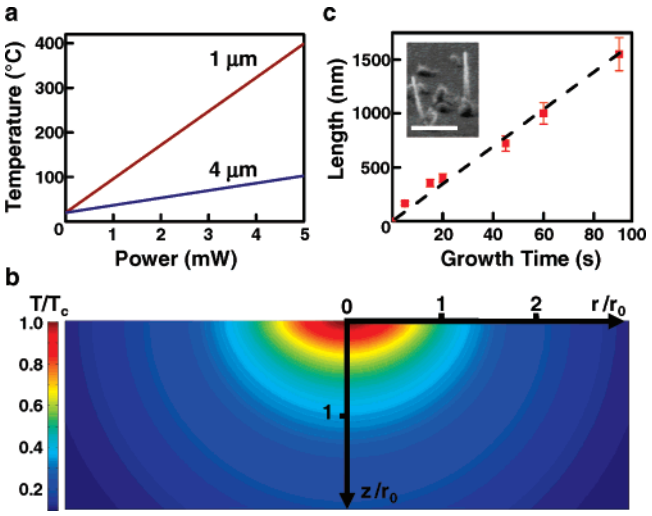

Figure 3. (a) Calculated temperature in the center of a gold nanoparticle layer illuminated with a 532 nm laser as a function of excitation power. Calculations for two illumination spot radii, r_0, of 1 and 4 μm are shown. The temperature was calculated with the thermal model described in the text. (b) Contour plot of the steady-state temperature distribution in the substrate as calculated with the same thermal model as in (a). All distances were normalized to r_0, and the temperatures were normalized to the highest temperature in the center of the illuminated region, T_C. (c) Dependence of the silicon nanowire length on the growth time appropriate to a SiH_4 pressure of 0.2 Torr and a 93 mW laser power focused into a 15.4 μm radius spot. The nanowire growth rate is somewhat adjustable by changing the precursor gas pressure and the laser power density. (Inset) SEM image of a typical silicon nanowire from which the nanowire length was determined (scale bar is 1 μm).

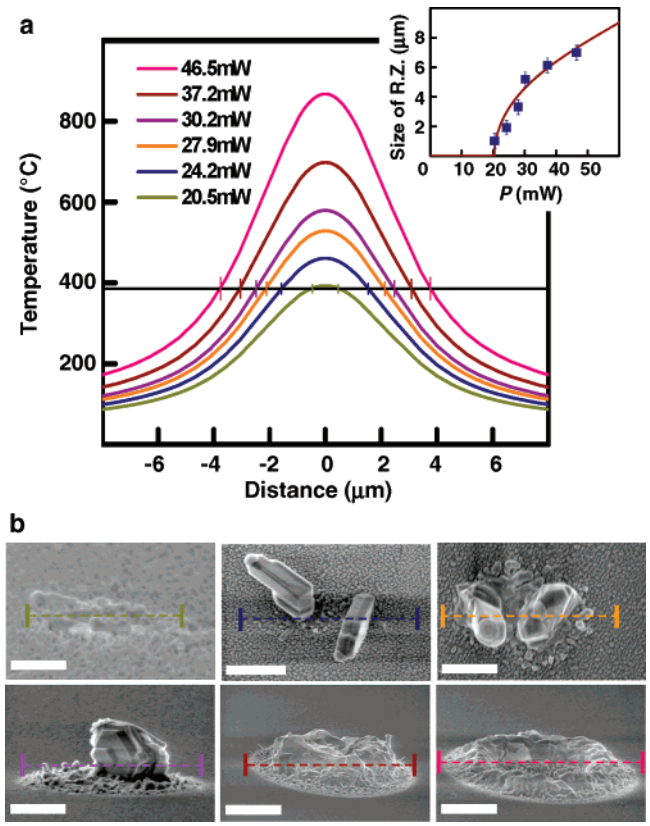

Figure 4. (a) Calculated temperature profiles at different illumination powers as denoted in the figure for a focused laser beam with fixed radius of 3.6 μm illuminating an assembly of gold nanoparticles. The temperature was calculated using the thermal model described in the text. The horizontal line marks the threshold temperature of 380 °C above which catalyzed Si deposition can occur, and the size markers (short vertical lines) indicate the predicted sizes for the deposits/reaction zones. The inset shows the calculated sizes of the RZs (solid line) obtained from the thermal model, along with the experimentally determined RZ diameters determined from the SEM images in (b) (blue data points) as a function of the laser power. A clear threshold value of ~20 mW is observed above which growth occurs. (b) SEM images of the silicon deposition by using the same illumination parameters as given for the calculation (marked with same color). For clarity, some are top view images while others are side views. The dashed lines with end-markers correspond to the theoretically predicted RZ sizes using the thermal model. Scale bars in the SEM images (from left to right) (upper) 300 nm, 500 nm, and 1.25 μm; (lower) 1.5, 2.0, and 2.0 μm.

to assemble NWs and NTs into complex device architectures. When the laser is turned on, a steady-state temperature profile will result in a time approximately equal to $t_s \approx r_0^2/D$. For the current experiments, the times are in the range of 10−100 μs. In experiments where well-separated nanoparticles are illuminated, steady-state will be reached even faster on 10 ps to 1 ns timescales. These short timescales suggest that this technique could be utilized to obtain a high degree of temporal control over the growth and chemical reaction kinetics with pulsed lasers. Experimental results indicate that under optimum growth conditions, the Si NW growth rate is about 1 micrometer per minute (Figure 3c). Compared to the typical nanowire growth time, the 10−100 μs control over the temperature will thus appear more-or-less instantaneous and the growth can in principle be stopped and started with submonolayer precision. This could have major implications for growth of one-dimensional heterostructures with a modulated composition for which precise control over layer spacing is desirable.[31,32]

The applicability of our thermal model is validated by correlating the calculated temperature distributions and deposition sizes obtained for a variety of laser powers at a fixed Gaussian spot size (Figure 4). The nature of the observed growth morphologies is analyzed in more detail in the Supporting Information (Figure S1). Using SEM, we found that deposition only occurs above a well-defined threshold power of about 20.5 mW (Figure 4b). From the temperature distribution curve calculated for this power, it follows that the Au nanoparticles need to reach a threshold temperature around 380 °C to catalyze growth (at 1.6 Torr pressure of silane), which is in good agreement with the threshold temperature of Au-catalyzed NW growth observed in conventional CVD experiments.[33] For all the plasmon-assisted NW and CNT growths, we found that threshold powers (i.e., temperatures) were in good agreement with those obtained in conventional CVD. When the laser power is increased above threshold, the size of the deposit/reaction zone (RZ) first increases rapidly and then finally tends to saturate (blue data points in the inset to Figure 4a). This evolution of the RZ with laser power can be explained quantitatively using our thermal model by realizing that the

size of the RZ at any laser power can be predicted by identifying the region in the temperature distribution that is above the threshold temperature for growth (colored horizontal markers in thermal distributions in Figure 4a and the corresponding SEM images in Figure 4b). The inset to Figure 4a shows the good agreement between the predicted sizes of the RZ (solid red line) and the experiments.

Although our thermal model is in good overall agreement with the experimental observations, it does not capture subtle phenomena related to the details of the exact nanoparticle size and spatial distributions. It is well established that random metal−dielectric composites can give rise to surface plasmon localization and strong electromagnetic field enhancements in deep subwavelength regions known as hotspots.[34] In such electromagnetic hot spots, the local high field intensity is expected to result in thermal hotspots due to the stronger local energy deposition. The repeatable growth of single nanostructures from random nanoparticle arrays may have been a direct result of the formation of such hotspots in the otherwise smooth temperature distribution. In the future, this type of surface plasmon and heat localization may well be exploited in carefully engineered light-concentrating structures to stimulate reactions with more precision in even smaller volumes than shown in the current study.

This research demonstrates that plasmon-assisted local temperature control provides an exciting route to gain a high degree of spatial and temporal control over CVD growth of semiconductor NWs or CNTs. It presents a process- and energy-efficient pathway for fabricating complex devices based on NWs or CNTs and offers significantly more flexibility than many conventional heating techniques, for example, based on running current through a thin wire. More generally, this newly acquired high level of control over nanoscale temperature fields may open up tremendous opportunities for engineers and scientists to initiate and control heat-assisted biochemical reactions, nanostructure deposition, and physical transformations and could enable the realization of a range of novel photothermal devices.

Acknowledgment. We thank D. Goldhaber-Gordon and J. Sulpizio for helping with the growth of carbon nanotubes. B. Wu, J.A. Schuller, T. Tauber, D.A. Boyd, L. Greengard, T. Defries, R. Verma, and K.A. DiZio are acknowledged for valuable discussions during different stages of the research and manuscript preparation. This work was supported by two DoD MURIs sponsored by the AFOSR (Gernot Pomrenke) on: "Electrically-Pumped, Silicon-Based Lasers for Chip-Scale Nanophotonic Systems" and "Plasmon Enabled Nanophotonic Circuits" and a gift from Greystoke Holdings.

Supporting Information Available: SEM image of a large silicon pillar surrounded by a band of Si nanowires obtained at a high (150 mW) laser power. Also, larger versions of some of the SEM images shown in this letter. This material is available free of charge via the Internet at http://pubs.acs.org.

References

(1) Chang, C. W.; Okawa, D.; Majumdar, A.; Zettl, A. *Science* **2006**, *314*, 1121.
(2) Schwab, K.; Henrlksen, E. A.; Worlock, J. M.; Roukes, M. L. *Nature* **2000**, *404*, 974.
(3) Ross, D.; Locascio, L. E. *Anal. Chem.* **2002**, *74*, 2556.
(4) Lyeo, H.; Khajetoorians, A. A.; Shi, L.; Pipe, K. P.; Ram, R. J.; Shakouri, A.; Shih, C. K. *Science* **2004**, *303*, 816.
(5) Clem, J. R. *Phys. Rev. Lett.* **1968**, *20*, 735.
(6) Hirsch, L. R.; Stafford, R. J.; Bankson, J. A.; Sershen, S. R.; Rivera, B.; Price, R. E.; Hazle, J. D.; Halas, N. J.; West, J. L. *Proc. Natl. Acad. Sci. U.S.A.* **2003**, *100*, 13549.
(7) Wong, N.; Kam, S.; O'Connell, M.; Wisdom, J. A.; Dai, H. *Proc. Natl. Acad. Sci. U.S.A.* **2005**, *100*, 4984.
(8) Huber, P. E.; Jenne, J. W.; Rastert, R.; Simiantonakis, I.; Sinn, H.; Strittmatter, H.; Fournier, D. V.; Wannenmacher, M. F.; Debus, J. *Cancer Res.* **2001**, *61*, 8441.
(9) Englander, O.; Christensen, D.; Lin, L. *Appl. Phys. Lett.* **2003**, *82*, 4797.
(10) Bondi, S. N.; Lackey, W. J.; Johnson, R. W.; Wang, X.; Wang, Z. L. *Carbon* **2006**, *44*, 1393.
(11) Abed, H.; Charrier, A.; Dallaporta, H.; Safarov, V.; Jamgotchian, H.; Tonneau, D. *J. Vac. Sci. Technol.* **2006**, *24*, 1248.
(12) ITRS International Technology Roadmap for Semiconductors; 2006. http://www.itrs.net/Links/2006Update/2006UpdateFinal.htm.
(13) Barnes, W. L.; Dereux, A.; Ebbesen, T. W. *Nature* **2003**, *424*, 824.
(14) Ozbay, E. *Science* **2006**, *311*, 189.
(15) Zia, R.; Schuller, J. A.; Chandran, A.; Brongersma, M. L. *Mater. Today* **2006**, 9, (20).
(16) Raether, H. *Surface Plasmons on Smooth and Rough Surfaces and on Gratings*; Springer-Verlag: New York, 1988.
(17) Kreibig, U.; Vollmer, M. *Optical Properties of Metal Clusters*; Springer: Berlin, 1995.
(18) Nitzan, A.; Brus, L. E. *J. Chem. Phys.* **1981**, *75*, 2205.
(19) Chen, C. J.; Osgood, R. M. *Phys. Rev. Lett.* **1983**, *50*, 1705.
(20) Boyd, D. A.; Greengard, L.; Brongersma, M.; El-Naggar, M. Y.; Goodwin, D. G. *Nano Lett.* **2006**, *6*, 2592.
(21) Fedotov, V. A.; MacDonald, K. F.; Zheludev, N. I.; Emel'yanov, V. I. *J. Appl. Phys.* **2003**, *93*, (6), 3540−4.
(22) Hu, M.; Chen, J.; Li, Z.; Au, L.; Hartland, G. V.; Li, X.; Marquez, M.; Xia, Y. *Chem. Soc. Rev.* **2006**, *35*, 1084.
(23) Jain, P. K.; El-sayed, I. H.; El-sayed, M. A. *Nano Today* **2007**, *2*, 18.
(24) Rontzsch, L.; Heinig, K. H.; Schuller, J. A.; Brongersma, M. L. *Appl. Phys. Lett.* **2007**, *90*, (4), 044105.
(25) Govorov, A. O.; Zhang, W.; Skeini, T.; Richardson, H.; Lee, J.; Kotov, N. A. *Nanoscale Res. Lett* **2006**, *1*, 84.
(26) Soares, B. F.; Jonsson, F.; Zheludev, N. I. *Phys. Rev. Lett.* **2007**, *98*, (15), 153905.
(27) Rao, A. M.; Richter, E.; Bandow, S.; Chase, B.; Eklund, P. C.; Williams, K. A.; Fang, S.; Subbaswamy, K. R.; Menon, M.; Thess, A.; Smalley, R. E.; Dresselhaus, G.; Dresselhaus, M. S. *Science* **1997**, *275*, 187.
(28) Maehashi, K.; Ohno, Y.; Inoue, K.; Matsumoto, K. *Appl. Phys. Lett.* **2004**, *85*, 858.
(29) Carslaw, H. S.; Jaeger, J. C. *Conduction of Heat in Solids*; Oxford University Press: Oxford, 1986.
(30) Burzo, M. G.; Komarov, P. L.; Raad, P. E. *IEEE Trans. Compon. Packag. Technol.* **2003**, *26*, 80.
(31) Yang, C.; Zhong, Z.; Lieber, C. M. *Science* **2005**, *310*, 1304.
(32) Wu, Y.; Fan, R.; Yang, P. *Nano Lett.* **2002**, *2*, 83.
(33) Kikkawa, J.; Ohno, Y.; Takeda, S. *Appl. Phys. Lett.* **2005**, *86*, 123109.
(34) Gresillon, S.; Aigouy, L.; Boccara, A. C.; Rivoal, J. C.; Quelin, X.; Desmarest, C.; Gadenne, P.; Shubin, V. A.; Sarychev, A. K.; Shalaev, V. M. *Phys. Rev. Lett.* **1999**, *82*, 4520.

NL0722370